



P-Wave Velocity Calculation (PVC) in Rock Mass Without Geophysical-Seismic Field Measurements

Mohammad Fathollahy¹ · Ali Uromeiehy² · Mohammad Ali Riahi³ · Yaghoob Zarei²

Received: 12 April 2020 / Accepted: 18 November 2020 / Published online: 1 January 2021
© Springer-Verlag GmbH Austria, part of Springer Nature 2021

Abstract

Ultrasonic studies have been used as low-cost, quickly updated, non-destructive techniques in geology and geo-technique. Conventional geophysical operations that allow measurements of wave velocity in rock mass are costly. In this study, we sought a strategy for calculation of wave velocity in rock mass without these field operations. The velocity of a wave in rock mass is a function of two major factors: the intact rock and joint properties. Wave velocity has the highest value in the intact rock, and decreases in the presence of joints, the poorer the conditions of the joints, the greater the decrease. Therefore, wave velocity can be predicted from a measurement of velocity in the intact rock and the properties of the joints. In this research, we first measured P-wave velocity in selected Andesite intact samples from the boreholes, and then measured the rate of effect of joint spacing, opening, orientation, infilling, and roughness on wave velocity by inducing joints in the rock. Afterwards, the orientations of the joints were recorded through surficial joint studies at 29 stations in field. Moreover, the characteristics of the underground joints (6,530 joints) were determined through geotechnical drillings along 9 boreholes (with a total length of 840 m). Finally, the velocity of the P-wave in the rock mass was calculated in field along the assumed profiles. For validation, we compared our velocity estimations with available field data along seven profiles with a total length of 644 m, coinciding with our assumed profiles. The calculated wave velocity and that measured through geophysical operation in field were in close agreement. Thus, wave velocity in rock mass could be computed at an approximation rate of about 10%.

Keywords P-wave · Velocity calculation · Rock mass · PVC

1 Introduction

It is widely known that wave velocity in rock mass is a function of two main factors, i.e., intact rock and discontinuities. The geo-mechanical properties of rock mass also follow the properties of intact rock and of the existing discontinuities. Accordingly, one can approximate the geo-mechanical properties of rock mass with the wave velocity at disposal and thereby avoid cost to determine the geo-mechanical parameters with direct experiments. Many researchers have tried to relate different fields such as the effect of various

properties of joints on wave velocity as well as the relationship between wave velocity and different dynamic parameters, among which the following cases can be referred to: use of ultrasonic techniques to determine the degrees of weathering and fracturing (Carvalho et al. 2010), assessment of the geotechnical properties of some rock materials (Yagiz 2011), evaluation of geomechanical properties (Sheraz et al. 2014; Yasar and Erdogan 2004), estimation of concrete strength (Hobbs and Tchoketch Kebir 2007; Trtnik and Kavčič 2009), and evaluation of joint anisotropy (Kano and Tsuchiya 2002). Moreover, an approximate relation between the petro-physical properties of rocks and P-wave velocity (V_p) has been shown by Del Rio et al. (2006) and Khandelwal and Ranjith (2010), and the relation between P-wave and S-wave velocity in dry and wet conditions in the sandstone of the Tuska region, Egypt was studied by Mohamed and Andreas (2015). Some investigations were focused specifically on the cracks in the rocks attempting to understand the relation between the P-wave velocity characteristics and the fracture properties. This plays a crucial

✉ Mohammad Fathollahy
m.fathollahy@uok.ac.ir

¹ Dept. of Earth Science, University of Kurdistan, Sanandaj, Iran

² Dept. of Engineering Geology, Tarbiat Modares University, Tehran, Iran

³ Institute of Geophysics, University of Tehran, Tehran, Iran

role in development of a certain number of physical models, demonstrating that the waveform, amplitude, and velocity of transmitted waves are greatly influenced by the manner and nature of the represented fractures, and also by the size, number, thickness, aperture, infilling, and other properties of the fractures (Sassa and Watanabe 1995; El Azhari and El Amrani 2013; Schoenberg 1980; Fehler 1982). The experimental studies by Kahraman (2002) on three types of naturally fractured rocks (i.e., Granite, Marble, and Travertine) showed that P-wave velocity decreases as fracture roughness coefficient (FRC) increases. Furthermore, the values of V_p depend on the hardness of the rocks, assessed by the rebound number of the Schmidt hammer (RN) and number of joints (JN). The results demonstrated that V_p decreases as joint number increases; moreover, the rocks with higher strength indicated a higher sound velocity index (SVI) (Kahraman 2001). Altindag and Guney (2005) studied the relationship between V_p and joint density (J), and confirmed the results obtained by Kahraman (2001), the decrease in V_p with the increase in the number of joints. Furthermore, they highlighted a good polynomial correlation between the number of joints and the reduction rate of V_p , showing that the P-wave velocities were rapidly attenuated with an increase in joint density. The experimental studies by El Azhari and El Amrani (2013) focused on two types of building stone (Calcarenite and Marble); the artificial joints created in the samples and the diminution of the P-wave was measured as a function of the orientation and number of joints. The results revealed that P-wave velocities undergo diminution, and their rates are highly dependent on the number of fractures and their orientations.

According to previous studies, Barton (2007) assessed the impact of different factors on attenuation of P-wave velocity and the relationship between velocity and geomechanical parameters. Altindag (2012) reviewed previous studies that had been conducted on sedimentary rocks, and the raw data of 97 samples were subjected to statistical analysis. The relationships between P-wave velocity and physical–mechanical properties were investigated using simple and multi-regression analysis methods. Fathollahy et al. (2015) measured the

effect of opening on P-wave velocity, and Fathollahy et al. (2017) evaluated the effect of joint spacing on P-wave velocity. They showed the diminution of the wave as well as joint number is dependent on joint spacing, where the diminution of the wave in joints with a spacing of 3 cm is more than in those with a spacing of 5 cm. Also other research was done to investigate the impact of saturation on seismic parameters and calculation of cementation in sandstone reservoir (El Sayed and El Sayed 2017, 2019).

It is common to measure wave velocity in rock mass on the field to approximate geo-mechanical parameters for design of engineering projects that are usually implemented in the phase of feasibility and the first phases of studies. Geophysical operation should be performed to obtain wave velocity, and requires time and cost consumption. We may save time and cost considerably if we can find a method to compute wave velocity without execution of geophysical operation, so that wave velocity in rock mass can be calculated through measurement of P-wave velocity in a few intact rock specimens in laboratory and recording of the characteristics of discontinuities on the field.

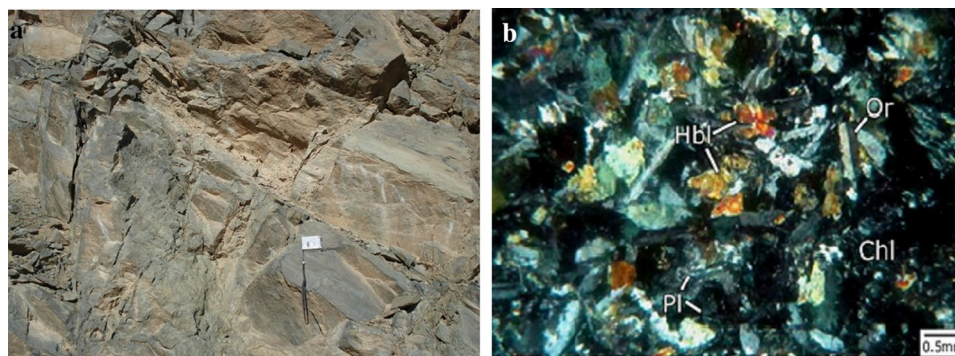
2 Method

The rock samples were selected from dark green Andesite units of Eosen in the Sanandaj-Sirjan zone in the northwest of Iran, which has been selected as a site for construction of a large dam about 120 m high.

This Andesite rock unit is an igneous rock that is classified as “good” in rock engineering classification point of view. Figure 1 shows a view of surface condition and petrographical characteristics of the rock.

The results of rock core samples from depths of 10–30 m boreholes around the dam axis were used in this research. Initially P-wave velocity was measured in intact specimens after transferring to the laboratory and preparing by cutting the ends and smoothing them. After the measurement of P-wave velocity in the intact samples, the share of each property in reduction of wave velocity was obtained through

Fig. 1 a Surface condition and b petrographical characteristics of the Andesite rock



creation of various conditions in the joints, including spacing, opening, infilling, orientation, and roughness (in natural mode), and wave velocity under each of the above conditions was measured and some formulae were obtained for each property. P-wave velocity was measured in the laboratory with an ultrasonic instrument known as Pundit Lab/Pundit Lab+, manufactured by Proceq, which complies with many standards (EN 12504-4 (Europe), ASTM C597-02 (North America), BS 1881 Part 203 (UK), ISO1920-7:2004 (International), IS13311 (India), and CECS21 (China)). The device includes two transducers (a transmitter and a receiver) that provide the ultrasonic waves. The transducers were applied on the two parallel faces of a rock specimen having a determined length (L) and trigger a series of ultrasound pulses. The device calculated the time interval (t) between the start and the reception of the pulses. The V_p in the specimen was calculated from the relation ($V_p = L/t$) and it was expressed in m/s.

Afterwards, the joint study was conducted on the field, and the geometric properties of the joints including the strike and dip were derived at the surface. Then, the geotechnical excavation was performed, and the properties of underground discontinuities were recorded and analyzed. In the next step, wave velocity was calculated along the assumed traversal profiles using the formulae obtained from the laboratory work; afterwards, velocity was measured with field geophysical operation along profiles adjusted to those mentioned above. Subsequently, the calculated velocity (i.e., that obtained using the formulae) was compared with the measured velocity (i.e., that obtained through field geophysical operation). It is noteworthy that the wave velocity measured by the refraction method was validated by the Downhole seismic technique. The Downhole test was conducted within

three boreholes down to a depth of 30 m. The results of the Downhole test confirmed those obtained by the refraction method. The overall research methodology, including the laboratory and field studies and, finally, a combination and comparison of them, is shown in Fig. 2.

3 Experimental Work

3.1 Determination of the Physical Properties of the Samples

To have a more complete understanding of the physical quality of intact rock, index experiments were performed on samples according to the ISRM standard. The results on some of the specimens are presented in Table 1.

3.2 P-Wave Velocity in Intact Rock

Through the tests conducted in laboratory on the specimens of intact rock, P-wave velocity was measured as 6085 m/s. The given velocity was assumed as base in the calculations of wave velocity (Table 2).

Although the rock is the same lithologically, the presence of microscopic structures such as micro-joints has caused the wave velocity not to be the same in all samples, however, to achieve real results, the mean of all samples has been considered in this research.

3.3 Effect of Joint Density on Wave Velocity

The number of joints and their spacing affect wave velocity. In a part of this research, the results of which have

Fig. 2 Method and steps of the research including two main parts: laboratory study (measurement of P-wave velocity in the intact rock and of the share of each joint property on wave velocity reduction) and field study (surface joint study for specification of orientation and geotechnical excavation for recording of the joint properties and geophysical operation for measurement of P-wave velocity on the field)

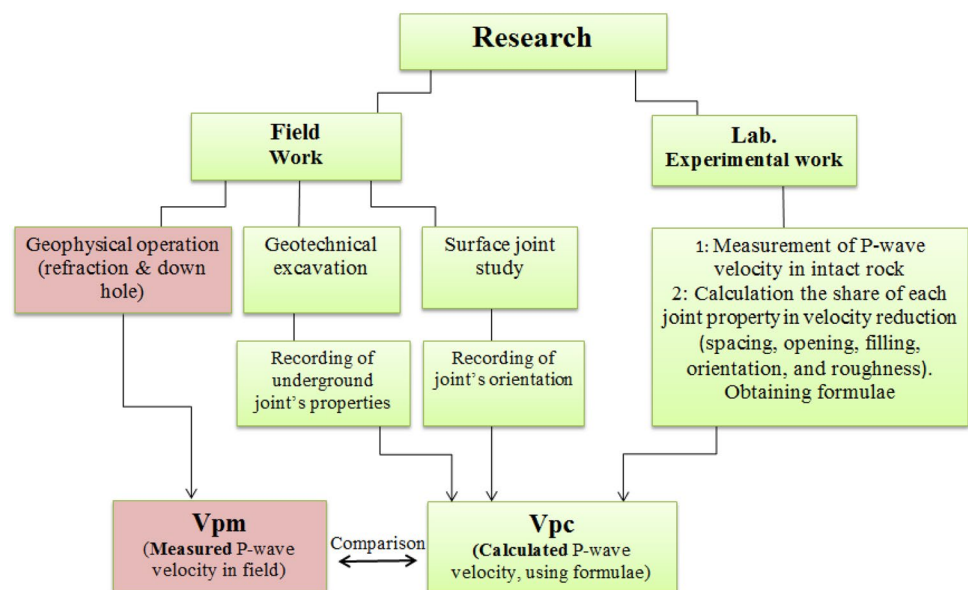


Table 1 Physical properties of the rock samples

Row	Saturated density (g/cm ³)	Dry density (g/cm ³)	n% (porosity)	W% (water absorption)	Row	Saturated density (g/cm ³)	Dry density (g/cm ³)	n% (porosity)	W% (water absorption)
1	2.98	2.97	0.97	0.33	16	2.97	2.96	0.84	0.28
2	2.93	2.92	1.27	0.43	17	2.93	2.92	1.27	0.43
3	2.95	2.94	1.04	0.35	18	2.9	2.89	0.97	0.33
4	2.95	2.94	1.05	0.36	19	2.92	2.91	0.97	0.33
5	2.9	2.89	0.97	0.33	20	2.89	2.88	0.82	0.29
6	2.97	2.96	0.84	0.28	21	2.97	2.96	1.07	0.36
7	2.97	2.96	1.07	0.36	22	2.95	2.94	1.37	0.46
8	2.95	2.94	1.37	0.46	23	2.95	2.94	1.05	0.36
9	2.89	2.88	0.82	0.29	24	2.95	2.94	1.05	0.36
10	2.92	2.91	0.7	0.33	25	2.96	2.95	1.06	0.35
11	2.92	2.9	1.12	0.39	26	2.95	2.94	1.04	0.35
12	2.98	2.97	0.97	0.33	27	2.98	2.97	0.97	0.33
13	2.92	2.9	1.12	0.39	28	2.93	2.92	1.27	0.43
14	2.94	2.93	0.95	0.33	29	2.95	2.94	0.9	0.32
15	2.95	2.94	1.04	0.35	30	2.9	2.89	0.97	0.33

Table 2 P-wave velocity in the intact rock samples

Row	V _p (m/s)	row	V _p (m/s)	row	V _p (m/s)
1	6060	14	6506	27	6335
2	5928	15	6614	28	6231
3	5786	16	6106	29	6311
4	6191	17	6011	30	6158
5	6300	18	5982	31	6502
6	6207	19	5933	32	6124
7	6261	20	6153	33	6034
8	5891	21	6017	34	5845
9	5845	22	6005	35	6128
10	4937	23	5805	36	6128
11	6174	24	6119	37	6128
12	6212	25	5722	38	6110
13	6300	26	6190	39	6060

Mean = 6085(m/s)

Average deviation of mean = 180

been published in Fathollahy et al. (2017), P-wave velocity was evaluated in different joint spacing, and the results demonstrated how the number and spacing of the joints influence P-wave velocity. They initially measured P-wave velocities in core specimen and then after generating artificial joints by cutting samples perpendicular to the core axis and coupling the samples. Measurements of V_p were performed according to the ASTM standard. They defined velocity reduction ratio (VRR %) to evaluate the variation of P-wave velocity by increasing the joint number with different spacing (Eq. 1).

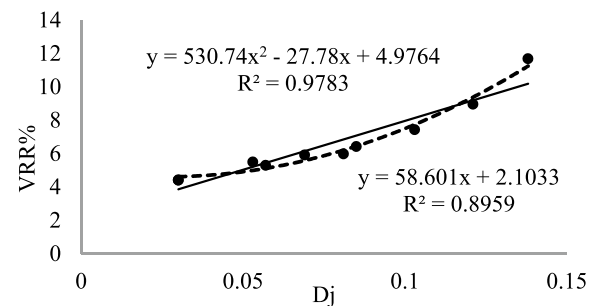


Fig. 3 Average of VRR% versus joint density (*D_j*) increasing in rock samples, results show VRR% increases with increasing of *D_j*

$$VRR\% = \frac{V_0 - V_1}{V_0} \tag{1}$$

where V₀ = initial P-wave velocity in sound specimen, V₁ = P-wave velocity in jointed specimen.

Results showed VRR% had an increasing trend for increasing joint number, but its rate was different for different joint spacing. The results showed VRR% value with a spacing of 5 cm, is more than spacing of 2 cm for the first three joints, but by increasing number of joints, the result is reversed. As seen the variation of P-wave velocity follows the density of the joints. Density of joint (*D_j*) was defined as the number of joints per unit of length in cm (Eq. 2).

$$D_j = \frac{\text{number of joints}}{\text{length (cm)}} \tag{2}$$

Table 3 Relation between VRR% and D_j in exponential and linear equation

Row	Equation	R -square (r^2)
1	Exponential $y = 530.74 \times 2 - 27.78x + 4.9764$	$R^2 = 0.978$
2	Linear $y = 58.601x + 2.1033$	$R^2 = 0.896$

$y = \text{VRR\%}$ (velocity reduction ratio) and $x = D_j$

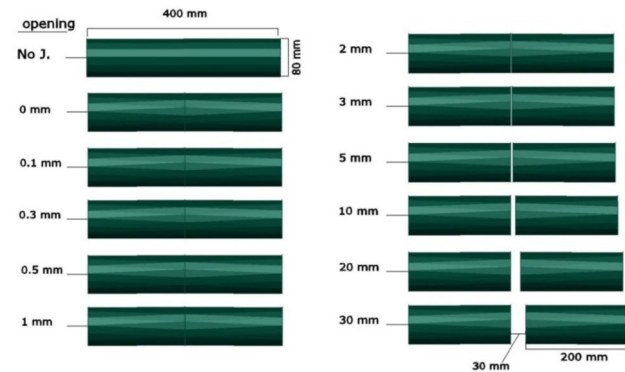


Fig. 4 Different opening (0, 1–30 mm) in the samples

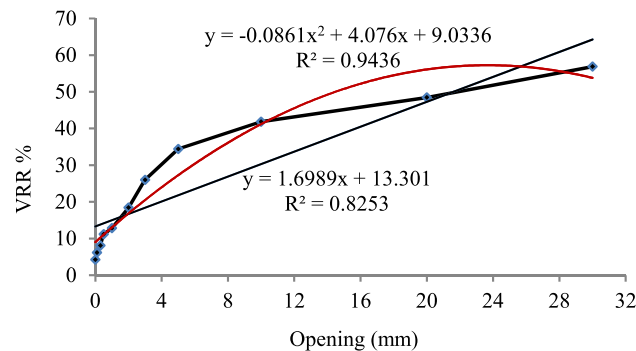


Fig. 5 Average VRR% versus opening in different sets of samples (Fathollahy et al. 2015)

Results showed VRR% had an increasing trend for increasing joint density (D_j) (Fig. 3).

As can be seen VRR% follows the D_s , and both linear and exponential relation between them is noticeable. Obtained equation is provided in Table 3.

3.4 Effect of Joint Opening on Wave Velocity

In another part of this research different openings were created and the effect of that, as a crucial parameter, on P-wave velocity was measured (Fig. 4). The results demonstrated that VRR% increases as does the opening. Figure 5 shows

Table 4 Relation between VRR% and opening in exponential and linear equations (Fathollahy et al. 2015)

Row	Equation	R -square (r^2)
1	Exponential $y = -0.0861x^2 + 4.076x + 9.0336$	$R^2 = 0.944$
2	Linear $y = 1.6989x + 13.301$	$R^2 = 0.825$

$y = \text{VRR\%}$ (velocity reduction ratio); $x = \text{opening (mm)}$

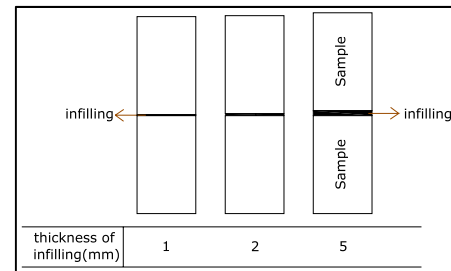


Fig. 6 Different thicknesses (0, 1, 2, and 5 mm) of Silica infilling in the samples

VRR% in different openings, and the obtained equation is provided in Table 4 (Fathollahy et al. 2015).

3.5 Effect of Joint Infilling on Wave Velocity

Infilling of joints was considered as another parameter in this research. Since the natural infilling of the rock mass on the field was Silica, it was selected as joint infilling in the laboratory. The sample preparation included the selection of homogenous samples and cutting and smoothing of their ends. After that, the joints were filled with Silica at different thicknesses of 1, 2, and 5 mm (Fig. 6) and for different coverage, and V_p was measured accordingly. The results showed an increase in P-wave velocity in all the sets with the increasing infilling thicknesses. Table 5 shows P-wave velocity versus the infilling thickness of Silica in joints with 100% and 0% (no infilling) coverage.

The results were analyzed using the method of least squares regression. The equation concerning the best model with R-square was obtained. The VRR% was correlated with the infilling values for the samples. The polynomial relationship (second degree) exhibited a good validity for Silica infilling (Fig. 7).

The regression equation and the R-square value are given in Table 6. Given the analysis, there is a strong relationship between VRR% and the infilling thickness values particularly with regard to a polynomial equation.

Similarly, as the joint surfaces on the field were not fully covered by Silica, the effect of coverage was analyzed as described in Table 7. The findings show that although

Table 5 Results of V_p measurement in samples with Silica infilling in 100% and 0% coverage

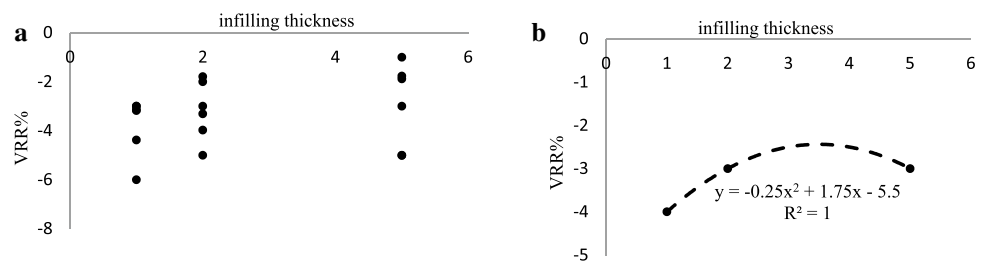
Samples	Infilling thickness (mm)	Infilling = 100%		Infilling = 0%
		V_p (m/s)	VRR%	V_p (m/s)
1,3	1	5628	-6	5304
2,4	1	5564	-3	5410
5,6	1	5567	-3	5425
7,8	1	5553	-4	5320
9,10	1	5601	-3	5430
11,12	1	5587	-3	5415
1,3	2	5563	-5	5304
2,4	2	5560	-3	5410
5,6	2	5554	-2	5425
7,8	2	5521	-4	5310
9,10	2	5494	-3	5318
11,12	2	5568	-2	5470
1,3	5	5584	-5	5304
2,4	5	5566	-3	5410
5,6	5	5503	-1	5425
7,8	5	5576	-5	5310
9,10	5	5563	-2	5460
11,12	5	5412	-2	5318

velocity is increased in the presence of filling, the results do not follow a certain general trend in line with the variation in coverage rate; thus, it may not be concluded that a rise in filling percentage could increase velocity further (Table 7).

3.6 Effect of Joint Dip on Wave Velocity

For determination of the variance of wave velocity upon passing joints at different dips, wave velocity was initially measured in samples without joints, some of which were then created at different angles (0° , 15° , 30° , 45° , 60° , and 90°) with respect to wave trend axis in specimens, and the velocities were measured after P-wave was passed through them (Fig. 8). The velocity derived from each sample was compared with the same primary velocity without joints for analysis of the results, and VRR% was obtained (Table 8).

Fig. 7 **a** Variation of VRR% versus infilling thickness in the samples and **b** relation between average VRR% and infilling thickness



The results of three series of data indicated that VRR% will be at maximum level if it is at the right angle (90° degrees), and it will be at minimum level if the angle is about 30° degrees. Overall, the value of VRR% shows an incremental trend as the angle rises (Fig. 9).

The regression equation and the R-square value are given in Table 9. Given the analysis, there is an acceptable relationship between VRR% and the joint dip values, particularly with regard to a polynomial equation.

3.7 Effect of Joint Roughness on Wave Velocity

The studies conducted by previous researchers have shown that joint roughness affects the speed of the passing wave. On that basis, some underground samples with natural joint roughness were selected from the excavated specimens for analysis of the effect of roughness on wave velocity. The samples were transferred to the laboratory with their normal state, and joint roughness was achieved using the profilometer (Barton Comb) and coefficient of roughness with respect to the ISRM standard (the form of joint roughness is shown visually in Fig. 10). It is noteworthy that the site under investigation includes homogeneous lithology with similar conditions in terms of roughness. This condition is visible in geotechnical drillings (Table 12); thus, the studied samples were assumed as the representative of the rock mass in site. The results indicated a decrease in velocity following the increase in roughness (Fig. 11).

The comparison of the given mean velocity of intact rock to that derived from jointed samples with natural joints indicated that such joints lead to a 14% decrease in wave velocity. Of course, part of this decrease in velocity is caused by the presence of discontinuity (joint plane),

Table 6 Regression equation and R-square coefficient in the Silica infilling

R-square (r^2)	Regression equation	Infilling type
$R^2 = 1$	$y = -0.25x^2 + 1.75x - 5.5$	Silica

$y = \text{VRR\%}$ (velocity reduction ratio); $x = \text{infilling thickness (mm)}$

Table 7 Effect of coverage percentage on VRR%





Infilling coverage %	VRR%	infilling thickness (mm)		
		1	2	5
25		-3.9	-3.3	-3.2
50		-3.2	-3.1	-3.1
75		-3.4	-2.9	-2.5
100		-3	-3.3	-3.0

Fig. 8 Joints with different dips (0°, 15°, 30°, 45°, 60°, 90°)

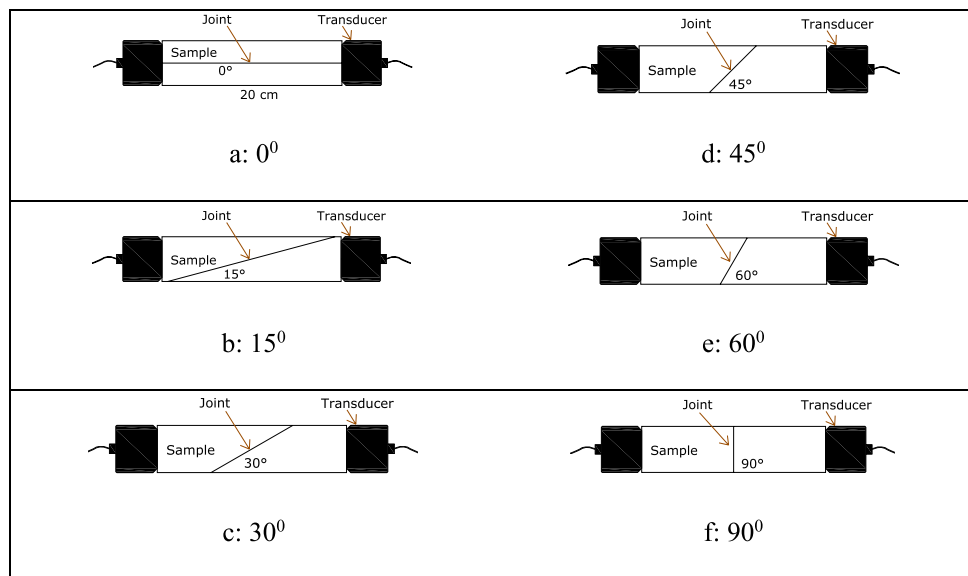


Table 8 P-wave velocity in the sound samples and those jointed with different dips

Average of V_p (m/s) in sound core	Dip of joint (degree)	Average of V_p (m/s) in jointed samples	VRR%
5771	0	5642	2.2
5702	15	5630	1.3
5520	30	5473	0.9
5567	45	5506	1.1
5975	60	5671	5.1
5780	90	5418	6.3

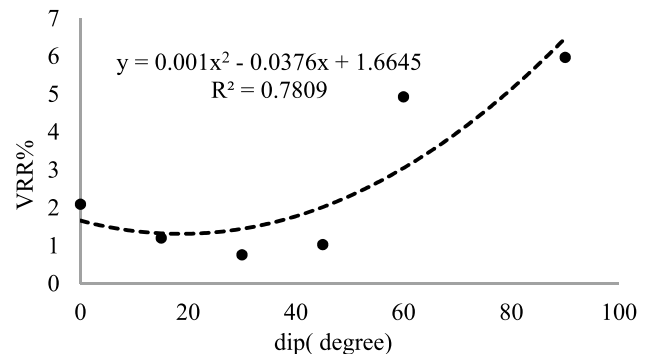


Fig. 9 VRR% versus joint dip (as can be seen, the VRR% value is maximal at 90° and minimal at about 30°)

another part concerns joint dip, and the other is caused by roughness. The role of roughness in reduction of velocity was identified given the above factors. As the angles existing in the samples are 40°–50° with the effect of about

2%, the role of infilling by –1%, and a joint plane may also reduce wave velocity by about 6%, roughness is expected to reduce wave velocity totally by about 7%. The initial

Table 9 Regression equation and *R*-square coefficient at different joint dips

<i>R</i> -square (<i>r</i> ²)	Regression equation
$R^2=0.781$	$y=0.001x^2-0.0376x+1.6645$

$y = \text{VRR\%}$ (velocity reduction ratio); $x = \text{joint dip}$ (degree)

velocity was decreased by this amount in the calculations of wave velocity in the rockmass.

4 Field Work

4.1 Joint Study

The surface joint studies were carried out at 29 stations (12 of them was used in this paper) to extract the

Fig. 10 Measurement of the joint roughness coefficient using the profilometer (Barton Comb), indicated step by step from *a* to *d*

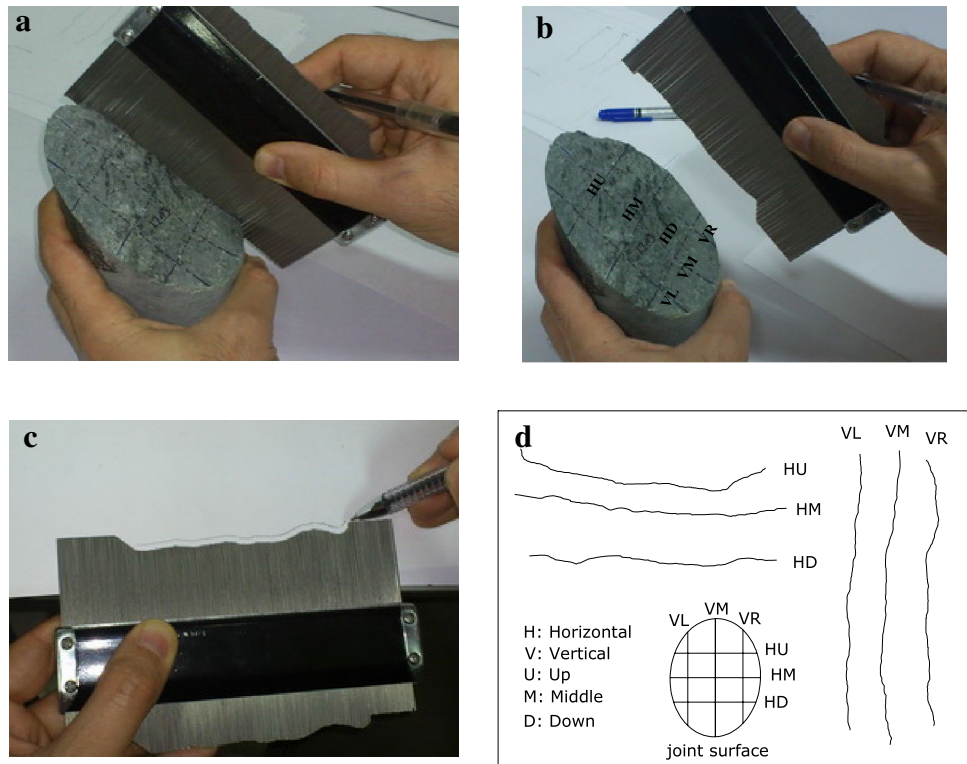
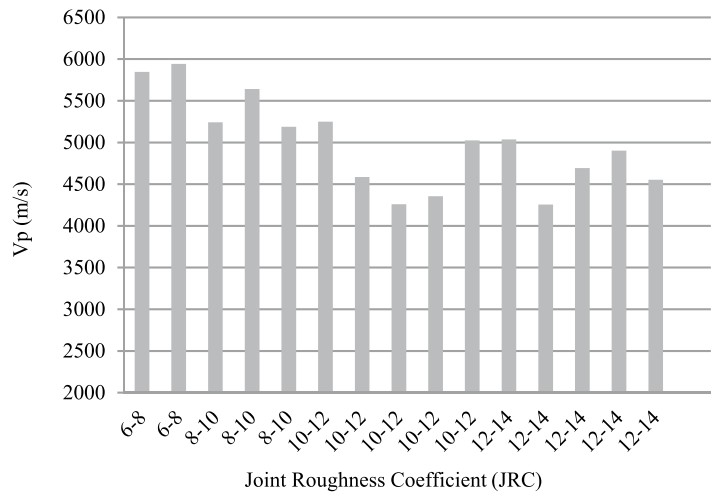


Fig. 11 JRC (joint roughness coefficient) versus P-wave velocity (as can be seen, velocity decreases as JRC increases)



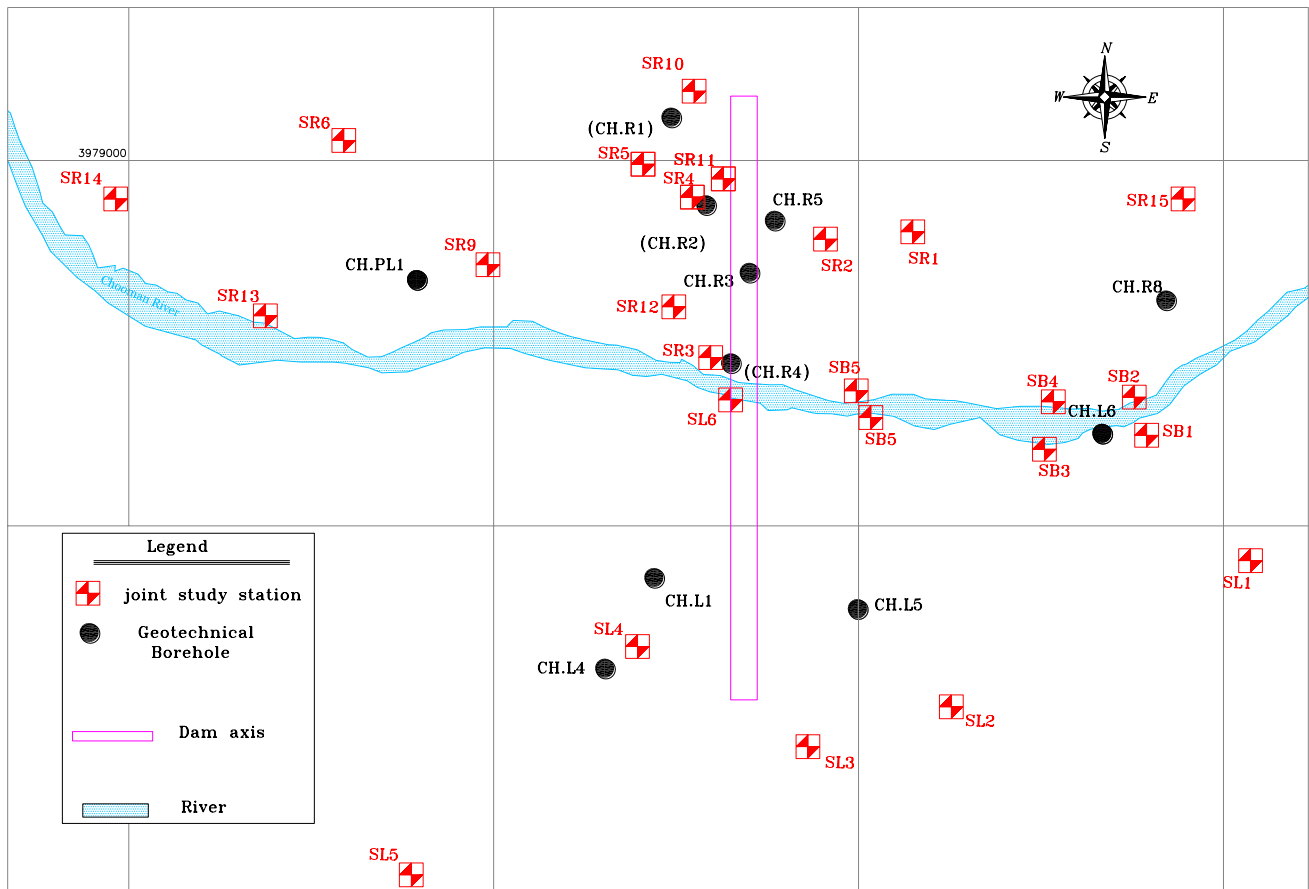


Fig. 12 Geotechnical borehole location and joint study station at field, where the circle symbol is geotechnical borehole and square symbol is joint study station

Table 10 Overall characteristics of surface joints at the 29 joint study stations

Number of station	Discontinuity	Dip	Dip direction	Opening (mm)	Spacing (cm)	Infilling	JRC	Overall main joints (Dip/Dip direction)
29 stations	J1	50	031	0-3	20-40	50% hard	8-14	
	J2	70	109	0-5	40-60	50% hard	10-14	
	J3	68	270	0-5	40-60	50% hard	10-14	

characteristics of joints at field. Although the surface information about joints such as weathering, opening, and filling are likely to be different from underground data, the orientations will be applicable to underground joints. Using the ISRM standard in this study, the properties of discontinuities were derived from different stations, and their characteristics were analyzed. The locations of the

stations and the results of the surface joint study are given in Fig. 12 and Table 10, respectively.

4.2 Geotechnical Excavation

A geotechnical operation was done for studying and acquiring information about the properties of underground

Table 11 Overall characteristics of the underground joints at 22 geotechnical boreholes

ROW	Borehole	Depth	Number of joint in bore-hole	Number of joint per meter in borehole	Number of joint per meter (from depth of 10 to 30 m)	Infilling type	JRC	Opening in depth of 10–30 m (m)
1	CHR-1	50	419	8.4	8.5	Silica	8–14	1>
2	CHR-2	120	877	7.3	7.6	Silica	8–14	1>
3	CHR-3	120	704	6	5.9	Silica	8–14	1>
4	CHR-4	100	754	7.5	6.8	Silica	8–14	1>
5	CHR-5	100	856	8.6	9.6	Silica	8–14	1>
6	CHR-6	120	1021	8.5	8.3	Silica	8–14	1>
7	CHR-7	100	718	7.4	7.1	Silica	8–14	1>
8	CHR-8	100	744	7.4	7.8	Silica	8–14	1>
9	CHR-9	74.5	503	7	9.1	Silica	8–14	1>
10	CHR-10	100	717	7.3	7.3	Silica	8–14	1>
11	CHR-11	105	1009	9.8	8.9	Silica	8–14	1>
12	CHPL-1	87.2	851	9.9	10.3	Silica	8–14	1>
13	CHL-1	50	268	5.5	5.5	Silica	8–14	1>
14	CHL-2	120	888	7.4	7.2	Silica	8–14	1>
15	CHL-3	100	765	7.9	7.1	Silica	8–14	1>
16	CHL-4	100	975	9.8	9.7	Silica	8–14	1>
17	CHL-5	100	775	7.8	10.3	Silica	8–14	1>
18	CHL-6	100	902	9	9	Silica	8–14	1>
19	CH2R-1	25	221	12.3	13.3	Silica	8–14	1>
20	CH2L-1	50	493	10.1	10	Silica	8–14	1>
21	CH2-L2	70	677	9.7	9.8	Silica	8–14	1>
22	PZL1	30	171	7.8	8.7	Silica	8–14	1>
Sum		1921.7	15,308					

joints. For this purpose, 22 boreholes (with a total length of 1922 m, that 9 boreholes with total length of 840 m were used in this research) were drilled using rotary techniques and perfect sampling, and the recovered cores were analyzed in them, with the joints studied and their properties recorded. Figure 12 shows the locations of the exploratory boreholes, and the underground joint properties are summarized in Table 11.

4.3 Evaluation of Different Parameters on P-Wave Velocity

As implied, the velocity of the P-wave in a rock mass is influenced by the intact rock and characteristics of discontinuities such as joint density, opening, infilling, dip, and roughness. Each factor affects velocity less or more under different conditions. The above parameters reduce wave velocity as compared to that in intact mode. The velocity calculated in the rock mass is obtained from deduction of velocity in the intact rock from the

cumulative effect of the parameters. P-wave was calculated along seven assumed profiles in site by using obtained formula in lab, surface study and geotechnical excavation. Details on the effect of each parameter in the present study are provided below.

4.4 Evaluation of the Effect of Joint Density (D_j) on P-Wave Velocity

Joint density is a factor effective on the velocity of waves. That is, a rise in the number of joints reduces velocity. The conducted studies have indicated that joint density (D_j) is directly related to decrease in wave velocity. This parameter was estimated by means of underground data in the path of the assumed profiles (and the effect was derived for each profile using the given formulae). For example, the geotechnical data on borehole CHR2, which is located near profile No. 3, were employed for estimation of D_j along the above profile, and the value was obtained as 0.075 (Table 13).

4.5 Evaluation of the Effect of Opening on P-Wave Velocity

The opening of joints at depth was assumed as 0.1 mm given the geological and structural conditions of the zone and low permeability of the rock mass at depth. VRR% was computed according to the derived formulae about the effect of opening on P-wave velocity (Table 13).

4.6 Evaluation of the Effect of Infilling on P-Wave Velocity

As mentioned in the previous sections, underground joints are filled with Silica, and are accumulated in joints mainly as unevenness in limited form. Trended changes were not observed in the findings based on the results of the analyses conducted in the laboratory on various thicknesses of Silica with different percentages of coverage. The presence of Silica in the joints in the laboratory tests exerted a change in VRR% of about -4% . Given the 0.1 mm thickness of filling underground and the equivalent coating of less than 25%, the value of VRR% was assumed as -1% based on the given formulae and engineering judgment about the method of filling.

4.7 Evaluation of the Effect of Joint Dip on P-Wave Velocity

The dip of joints was recorded in joint-studying stations within the surface adjacent to the profiles for analysis and calculation of the effect of the dip of joints on wave velocity in field (using the formulae derived in lab). Figure 13 shows the positions of profile PR3 and joint-studying stations SR5 and SR4 and the location of borehole CHR2. The data extracted from the above stations were employed for finding the strike and dip of the joints. With respect to the axis of profile PR3, the incidence angle between the wave and the joints was acquired after the average of the joints was recorded and calculated, and the effect on the decrease in velocity was calculated.

Table 12 presents the joint sets in stations SR4 and SR5 and the method of summing up and calculating the apparent dip with respect to the direction of profile 3.

This operation was carried out for all the profiles and the results were used in the relevant parts.

4.8 Evaluation of the Effect of Joint Roughness

As implied, wave velocity is reduced as roughness increases. The observed difference in velocity between intact samples and those with natural joints is due to the effective factors, including presence of joints, dip, and roughness. Given the role of a joint in the reduction of velocity by up to 6%, the role of infilling by -1% , and the role of dip by 2%, the role of roughness in the reduction of velocity in the examined rock was derived. Under different conditions, the calculated value of VRR% was estimated as 7 for profile No. 3 using the underground data from borehole CHR2 at depth 10–30 m.

4.9 P-Wave Velocity Calculations (PVC)

The value of VRR% was calculated for each of the parameters, and the sum was obtained. For this purpose, the properties of the underground joints were extracted, their orientations were recorded given the alignment of the seismic profile, and the effect of each parameter on the reduction of wave velocity was exerted (aided by the formulae derived in lab). On that basis, rock mass velocity at field was calculated through subtraction of the total reduction from velocity in the intact rock (Table 13).

This operation was carried out for the all profiles and the results are presented in Table 14.

5 Geophysical Operations

The seismic studies of the refractive method were conducted along seven profiles (coincident to assumed profiles were mentioned before) for recording P-waves using the source of mechanical energy. Propagation velocity was determined

Fig. 13 Locations of the joint-study stations (SR4, SR5), seismic profile (PR3), and geotechnical borehole (CHR2), (green lines are joints measured in SR4 and SR5 which are shown in stereonet)

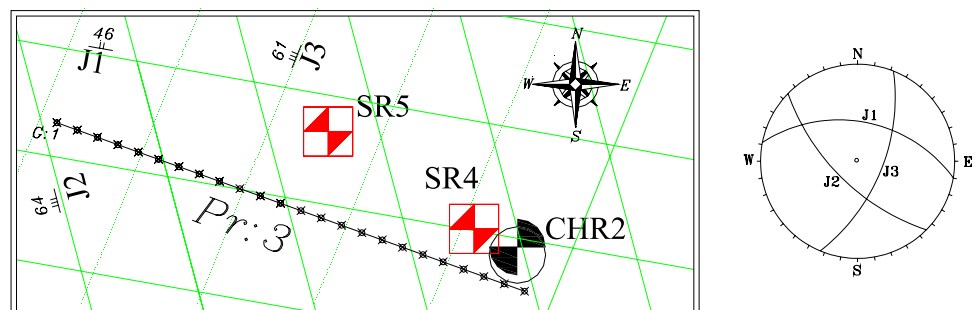


Table 12 Calculation of apparent joint dip with respect to the wave path along PR3 (there are three joint sets in each station: J1, J2, and J3, which are one-to-one equations)

Joint study station	Joint set	Dip (degree)	Dip direction	Rep. joint set	Average of dip	Average of dip direction	Average of joint strike	Strike of seismic profile	Apparent dip	Average of apparent dip
SR4	J1	37	15							
	J2	85	230							
	J3	50	80	J1	46	10	100	110	10	43.4
SR5	J1	55	5	J2	64	255	345		59	
	J2	43	280	J3	61	112	202		61	
	J3	72	143							

within earth layers down to a depth of 40 m approximately through repetition of the impacts of the wave source and reception of waves by the seismometer. The Pick-Win software was used for processing the recorded waves and for determining the times of their reception. As observed, the seismographic profiles, exploratory boreholes, and joint study stations are located within the limits of the dam axis (Fig. 14). As three classes of information (surface studies, geotechnical excavation, and geophysical studies) are required for interpretation and analysis, the results derived from those profiles (profiles No. 3, 4, 5, 14, 18, 22, and 23) were used, overlapping exploratory boreholes and joint study stations. Also Downhole method test was conducted in three boreholes (DH1, DH2 and DH3) to validate refraction method and confirm it. The results on the geophysical profiles are presented in Table 15.

Two geophysical layers were recognized through seismographic operation with the refraction method at a depth of about 40 m. The first layer is composed of debris and the weathered part of the rock, where thickness is less than 10 m at all points. The second layer includes the intact part of the rock, which is located under the first. Given the above issues, P-wave velocity was considered in the sound part of the rock (second layer), and the utilized geotechnical data were designated within a depth of 10–30 m.

6 Discussions

Calculating (using data and relation) and measuring (using geophysical method) velocity demonstrated that the calculated velocity and that measured in field were considerably close to each other. Specifically, the statistical computations indicated a variance range of 7–13%, i.e., a mean of 10% and an average deviation of mean value of 3 (Table 16). Figure 15 shows the variances of measured velocity (V_{pm}) and calculated velocity (V_{pc}). As can be seen, these two velocities have generally similar trends, where V_{pc} decreases or increases as does V_{pm} . Though V_{pm} and V_{pc} are reasonably close to each other, they are not completely compatible, due to unknown factors such as microscopic structures and other heterogeneities. The results show that it can be calculated with approximately 10% of the wave velocity in the rock mass. Statistical analysis based on linear regression models for the data also approves the strong linear relation between V_{pm} and V_{pc} . The fitted model is $V_{pm} = 0.906 \times V_{pc}$ and considering the ANOVA table, $R^2 = 0.99$ and Sig. = 0.000 which implies that the model is strongly significant.

Table 13 P-wave velocity calculation along PR3 with respect to all the effective parameters

P wave Velocity Calculation									
profile No.		Azimuth		Stations		Borehole			
3		110		SR4, SR5		CHR2			
Joint density (Dj)		Opening (mm)		Infilling (mm)		Joint dip (degree)		Roughness	
Value	VRR%	Value	VRR%	Value	VRR%	Value	VRR%	JRC	VRR%
0.075	5.88	0.1	6.2	0.1	-1	43.4	1.91	8-14	7
Vp in intact rock (m/s)			VRR% (Total)	Vp Calculated (m/s)		Vp Measured in rock mass in field by geophysical operation (m/s)			
6085			19.99	4869		4300			

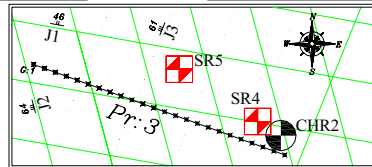


Table 14 Calculated V_p (V_{pc}) along assumed profiles

V_{pc} (calculated by obtained relations)	VRR% (velocity reduction ratio)	Reference velocity (m/s)	Profile No
4869	19.99	6085	Pr:3
4588	24.62		Pr:4
4915	19.25		Pr:5
4602	24.4		Pr:14
4682	23.08		Pr:18
4703	22.72		Pr:22
4588	24.62		Pr:23

7 Conclusions

This study explored the possibility of calculating P-wave velocity without any geophysical operations by obtaining the impact rate of the factors effective on wave propagation velocity in rock mass. To this end, the underground parts of the rock mass (depth 10–30 m) were initially sampled, and P-wave velocity in the intact rock was primarily measured in a laboratory. Then, the effects of the density, opening, infilling, dip, and roughness of the joints were examined through creation of artificial joints in the samples, and an impact rate was thus obtained.

Afterward, the orientations (strike and dip) of the joints were obtained by surface joints studies in field, and their underground characteristics were recorded using geotechnical data. Then, wave velocity in the rock mass was calculated along the assumed profiles, coinciding with available seismic profiles. The following results were obtained.

1. Wave velocity in rock mass can be computed without geophysical-seismic field measurements through extraction and recording of the properties of joints and P-wave velocity in the intact rock.
2. Different properties of the joints affect wave velocity differently. The rates of their effects may be measured through physical stimulation of joints.
3. The comparison between V_{pc} and V_{pm} indicated that the two velocities are considerably consistent with each other, where mean difference and deviation from the mean are 10% and 3, respectively.

Obtained results are limited to this hard rock facies in its geologic province, thus we suggest that similar research be carried out on different rock types with different joint characteristics for a more comprehensive evaluation of the relationship between V_{pm} and V_{pc} .

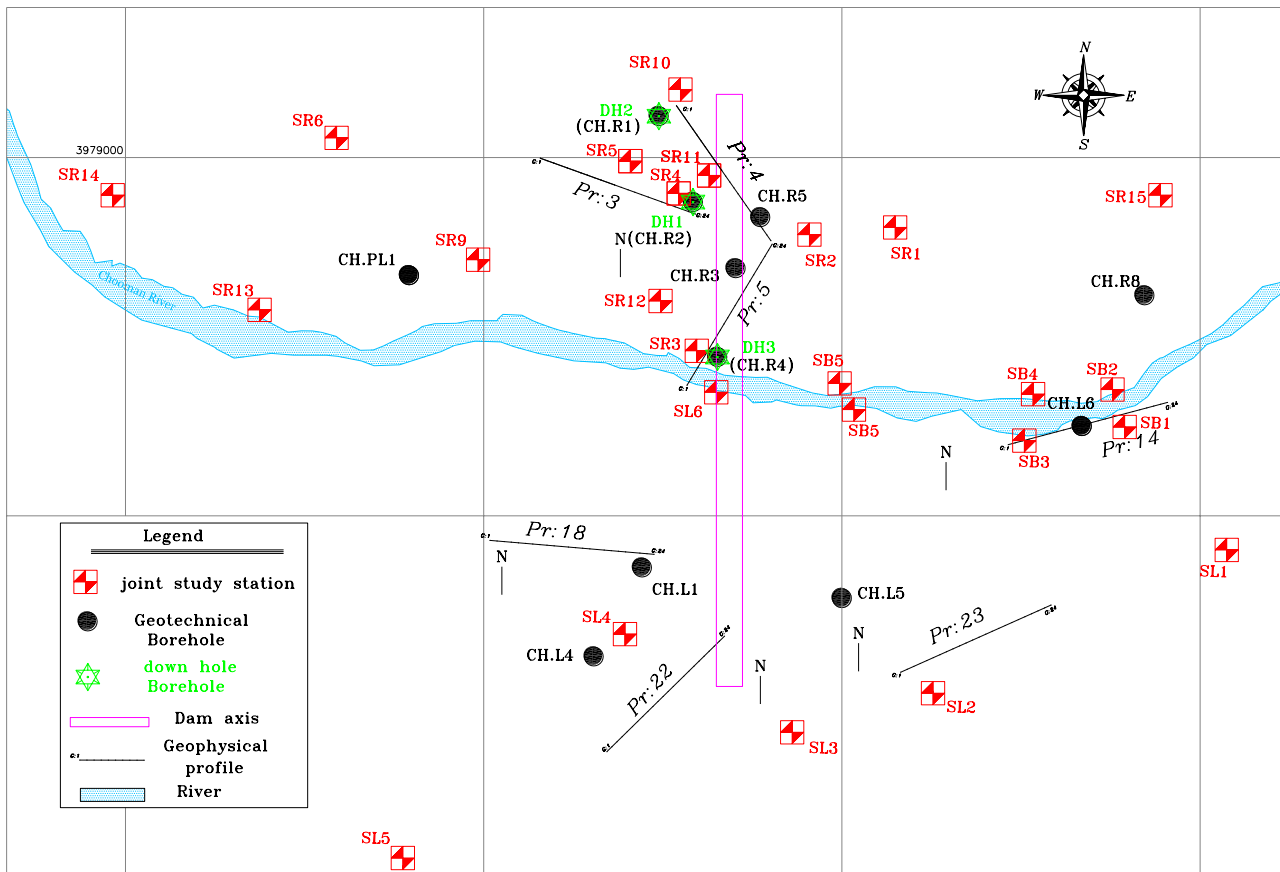


Fig. 14 Seismic profiles, Joint study station and geotechnical boreholes (where marked line is geophysical profile, the square symbol is joint study station, circle symbol is geotechnical borehole and star symbol is Downhole test location)

Table 15 Underground geology layers according to the geophysical operation

Profile number	Layers	Depth of sound rock (m)	P wave velocity in sound rock (m/s)
Pr:3	2	3.5	4300
Pr:4	2	10	4050
Pr:5	2	3	4350
Pr:14	2	4	4250
Pr:18	2	4	4200
Pr:22	2	5	4400
Pr:23	2	4	4300

Table 16 Comparison of calculated V_p (V_{pc}) with measured V_p (V_{pm})

$\left(\frac{V_{pc}-V_{pm}}{V_{pm}}\right)100$	V_{pm} (measured in field by geophysical operation)	V_{pc} (calculated by obtained relations)	Profile no
	4300	4869	Pr:3
	4050	4588	Pr:4
	4350	4915	Pr:5
	4250	4602	Pr:14
	4200	4682	Pr:18
	4400	4703	Pr:22
	4300	4588	Pr:23

Average = 10

Range = 6

$A_{DM} = 3$

A_{DM} average deviation of mean

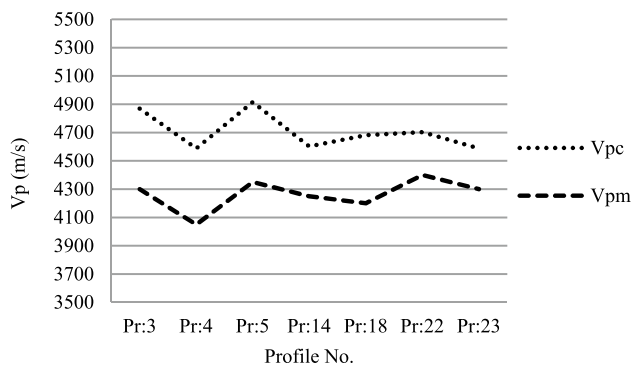


Fig. 15 Comparison of the calculated and measured P-wave velocity (the dotted line represents calculated V_p (V_{pc}), and the dashed line shows measured V_p (V_{pm}); their total behavior is similar, as can be seen)

Acknowledgements The authors would like to acknowledge the collaboration made by Iran Water and Power Resources Development Company, Sad Tunnel Pars Company, and the Institute of Geophysics of Tehran University.

Data Availability All the data, models, and codes generated or used during the study appear in the submitted article.

References

- Altindag R (2012) Correlation between P-wave velocity and some mechanical properties for sedimentary rocks. *J South Afr Inst Min Metall* 112:229–237
- Altindag R, Guney A (2005) Evaluation of the relationships between P-wave velocity (V_p) and joint density (J). In: *The 19th international mining congress and fair of Turkey IMCET*, Izmir, June 09–12, pp 101–106
- Barton N (2007) *Rock quality, seismic velocity, attenuation and anisotropy*. Taylor & Francis/Balkema
- Carvalho JP, Pinto C, Lisboa JV, Sardinha R, Catrapona A, Borges J, Tlemçani M (2010) Assessing the degree of fracturing and weathered layer thickness using seismic and GPR data. In: *72nd EAGE conference and exhibition incorporating SPE EUROPEC* Barcelona, Spain
- Del Rio LM, Lopez F, Esteban FJ, Tejado JJ, Mota M, González I, San Emeterio JL, Ramos A (2006) Ultrasonic characterization of granites obtained from industrial quarries of extremadura (Spain). *Ultrasonics* 44:e1057–e1061. <https://doi.org/10.1016/j.ultras.2006.05.098>
- El Azhari H, El Amrani El Hassani IZ (2013) Effect of the number and orientation of fractures on the P-wave velocity Diminution: Application on the building stones of the Rabat Area (Morocco). *Geomaterials*. <https://doi.org/10.4236/gm.2013.33010>

- El Sayed AMA, El Sayed NA (2017) Impact of reservoir fluid saturation on seismic parameters: Endrod Gas Field. *Earth Environ Sci* 95:032028. <https://doi.org/10.1088/1755-1315/95/3/032028>
- El Sayed AMA, El Sayed NA (2019) Calculation of cementation exponent and multiplier using P wave velocity and porosity for sandstone reservoirs. *Earth Environ Sci* 362:012001
- Fathollahy M, Uromeiehy A, Riahi M A, Bashirgonbadi M (2015) Effect of joint opening on P-wave velocity measurement in Andesite rock samples. In: *Seventh international conference on seismology and earthquake engineering*, Tehran, Iran
- Fathollahy M, Uromeiehy A, Riahi MA (2017) Evaluation of P-wave velocity in different joint spacing. *Boll Geofis Teor Appl* 58(3):157–168. <https://doi.org/10.4430/bgta0208>
- Fehler M (1982) Interaction of seismic waves with a viscous liquid layer. *Bull Seismol Soc Am* 72(1):55–72
- Hobbs B, Tchoketch Kebir M (2007) Non-destructive testing techniques for the forensic engineering investigation of reinforced concrete buildings. *Forensic Sci Int* 167:167–172
- Kahraman S (2001) A correlation between P-wave velocity, number of joints and Schmidt hammer rebound number. *Int J Rock Mech Min Sci* 38(5):729–733. [https://doi.org/10.1016/S1365-1609\(01\)00034-X](https://doi.org/10.1016/S1365-1609(01)00034-X)
- Kahraman S (2002) The effects of fracture roughness on P-wave velocity. *Eng Geol* 63(3–4):347–350. [https://doi.org/10.1016/S0013-7952\(01\)00089-8](https://doi.org/10.1016/S0013-7952(01)00089-8)
- Kano S, Tsuchiya N (2002) Parallelepiped cooling joint and anisotropy of P-wave velocity in the Takidani granitoid, Japan Alps. *J Volcanol Geoth Res* 114:465–477
- Khandelwal M, Ranjith PG (2010) Correlating index properties of rocks with P-wave measurements. *J Appl Geophys* 71(1):1–5. <https://doi.org/10.1016/j.jappgeo.2010.01.007>
- Mohamed AK, Andreas W (2015) Study on P-wave and S-wave velocity in dry and wet sandstones of Tushka region. *Egypt Egypt J Petrol* 24:1–11
- Sassa K, Watanabe T (1995) Velocity and amplitude of P-waves transmitted through fractured zones composed of multiple thin low-velocity layers. *Int J Rock Mech Min Sci Geomech Abstr* 32(4):313–324. [https://doi.org/10.1016/0148-9062\(95\)00008-5](https://doi.org/10.1016/0148-9062(95)00008-5)
- Schoenberg M (1980) Elastic wave behavior across linear slip interfaces. *J Acoust Soc Am* 68(5):1516–1521. <https://doi.org/10.1121/1.385077>
- Sheraz AM, Emad MZ, Shahzad M, Arshad SM (2014) Relation between uniaxial compressive strength, point load index and sonic wave velocity for Dolorite. *Pak J Sci* 66(1):60–66
- Trtnik G, Kavčič F TG (2009) Prediction of concrete strength using ultrasonic pulse velocity and artificial neural networks. *Ultrasonics* 49:53–60
- Yagiz S (2011) P-wave velocity test for assessment of geotechnical properties of some rock materials. *Bull Mater Sci* 34:947–953
- Yasar E, Erdogan Y (2004) Correlating sound velocity with the density, compressive strength and Young's modulus of carbonate rocks. *Int J Rock Mech Min Sci* 41:871–875

Publisher's Note Springer Nature remains neutral with regard to jurisdictional claims in published maps and institutional affiliations.